Progress in Physics of Applied Materials 2 (2022) 83–92

Semnan University

Progress in Physics of Applied Materials

journal homepage: https://ppam.semnan.ac.ir/

Fabrication, characterization, and photocatalytic degradation of malachite green by CuO nanocatalyst

Leila Kafi-Ahmadi*[1], Shahin Khademinia[2]

[1]*Department of Inorganic Chemistry, Faculty of Chemistry, Urmia University, Urmia, Iran*
[2]*Department of Inorganic Chemistry, Faculty of Chemistry Semnan University, Semnan 35351-19111, Iran*

ARTICLE INFO

Article history:
Received: 14 July 2022
Revised: 30 November 2022
Accepted: 3 December 2022

Keywords:
CuO
Solid state
MG
Wastewater
Nanomaterial

ABSTRACT

Solid state synthesis of CuO nanophotocatalyst is reported in the present work using copper salts raw materials at 600 ºC for 5 h. X-ray powder diffraction (XRPD) technique was used to characterize the prepared nanomaterials. Rietveld analysis data confirmed the high purity of the prepared samples. The XRD data showed that the peaks belong to monoclinic structure with a space group of C2/c. The Rietveld data indicated that the cell parameters are a=4.68244, b=3.42366, c=5.12641 Å and β=99.46º for S_1, a= 4.68073, b=3.42521, c=5.13221 Å and β=99.36º for S_2 and a=4.68233, b=3.42396, c=5.12941 Å and β=99.30º for S_3. The morphology of the prepared samples was investigated by FESEM technique. The FESEM images showed that the synthesized CuO compounds had particle morphology with the particle size of 22–50 nm. The photocatalytic performance of the obtained target was studied to degrade malachite green (MG) from wastewater solution.

1. Introduction

CuO is a compound with p-type semiconductor behavior and finds significant considerations due to its great physical and other attractive properties. CuO has direct band gap energy of 1.2 eV that is broadly utilized in different applications including catalysis [1], sun powered vitality transformation [2], gas sensor [3], and field emission [4]. Copper-oxygen framework contains two stable stoichiometric oxides, cuprous (Cu_2O) and cupric (CuO) oxides. Cuprous oxide contains a cubic crystal structure with a band gap in the range of 2.0–2.5 eV, though cupric oxide has a monoclinic crystal structure with a lower band gap energy value [5]. However, these novel properties can be attributed to the CuO nanostructures that appear the novel properties comparing to bulk sample. Nanostructures of CuO are synthesized in several methods. Within the past decades, various strategies have been proposed to synthesize CuO nanoparticles with different sizes and shapes such as warm oxidation [6], sonochemical [7], combustion [8], quick-precipitation [9,10], processing [11], electrodeposition [12], sonochemical amalgamation [13], ultrasonic pyrolysis [14], precipitation [15,16], etc. In any case, solid state rout is one of the best and broadly utilized strategies for creating different types of materials for different applications [17, 18]. Malachite green (MG) is a non-biodegradable dye pollutant and has now become a highly controversial compound to the consumers of treated fish, including its effects on the immune and reproduction systems. It should not be used for beverages, food, and medicines because it causes skin irritation, blurred vision or cause interference. Its inhalation may cause irritation to the respiratory tract, and in large quantities can cause tissue damage and inflammation of kidneys [19-25]. Due to the above information about the hazardous of the dye compound, we decided to study the photocatalytic degradation of MG in the present study.

Photocatalytic degradation of pollutants has been previously done by metal oxides nanomaterials [26-45]. Experimental design method is utilized to discover optimum values of parameters affect the MG photodegradation conditions. Within the method, a design of expert (DOE) utilizing Central Composite design (CCD) is used. Design of expert offers computer produced D-optimal designs for cases where standard designs are not appropriate, or where we wish to increase an existing

* Corresponding author. Tel.: +98443255294
E-mail address: L.kafiahmadi@urmia.ac.ir

DOI: 10.22075/ppam.2022.27812.1033

design [45, 46]. On the off chance that the separate from the center of the plan space to a factorial point is ±1 unit for each figure, the remove from the center of the plan space to a point is |α| > 1 [45, 46]. The most reason of the present work is presenting a productive photocatalyst for degradation of MG water pollutant. Moreover, the photocatalytic performance of the synthesized CuO nanomaterial is explored for the degradation of MG under blue light. Design expert method is utilized to optimize variables influencing the degradation response.

2. Methods and characterization

All chemicals were of analytical grad, obtained from commercial sources, and utilized without further refinement. The morphology of the obtained materials was studied with a field emission scanning electron microscope (Hitachi FE-SEM show S-4160). The computer program utilized for design of expert (DOE) was experimental design 7. The photocatalytic performance of the synthesized CuO sample for the degradation of MG was measured using H_2O_2 (30%, w/w) under blue light illumination. Design expert software data revealed that the optimum conditions for the degradation of MG were 0.02 g catalyst, 0.05 mL H_2O_2, and 35 min reaction time. The degradation efficiency was 78 %. The concentration and volume of MG solution were 100 ppm and 80 mL, respectively. The light was illuminated by a 40 W power white color fluorescent lamp. The illumination intensity amount was 1.5 W/m^2 that was measured by a digital lux meter.

2.1. Catalyst preparation

In a typical solid state synthesis experiment, 0.18 g (1 mmol) of Cu $(CH_3COO)_2$ (Mw = 181.6 gmol^{-1}) (S_1) or 0.24 g (1 mmol) of $Cu(NO_3)_2.3H_2O$ (Mw = 241.6 g mol^{-1}) (S_2) or 0.25 g (1 mmol) of $CuSO_4.5H_2O$ (Mw = 249.7 gmol^{-1}) (S_3) were powdered. The powder was poured into a 25 mL crucible and heated in an electrical furnace in one step at 600 °C for 8 h. The crucible was allowed to be cooled normally to the room temperature in the furnace.

3. Results and discussion

3.1. Characterization

The crystal structure of the obtained nanomaterials was examined by Rietveld examination utilizing XRPD information. Figure 1 (a-c) outlines the examination of the obtained XRPD information on a scale of 2θ to 10-90°. The red lines indicate the watched power and the black lines are the calculated information; additionally, the blue lines demonstrate the distinction between the observed and computed values. The data showed that the peaks belong to monoclinic structure with a space group of C2/c. The Rietveld data indicated that the cell parameters are a=4.68244, b=3.42366, c=5.12641 Å and β=99.46º for S_1, a= 4.68073, b=3.42521, c=5.13221 Å and β=99.36º for S_2 and a=4.68233, b=3.42396, c=5.12941 Å and β=99.30º for S_3. The diffraction peaks at 32.55, 35.64, 38.85, 48.88, 53.47, 58.27, 61.68, 65.74, 66.27, and 67.87° are corresponded to (110), (002), (111), (-202), (020), (202), (-113), (022), (-311), and (113) Bragg planes.

3.2. FESEM images

Fig. 2 a-f presents FESEM images of the as-prepared CuO nanomaterial. The images show that the synthesized CuO compounds have particle morphology with the particle size of 22–50 nm. It is clear that changing the raw materials type does not affect the morphology type. However, it shows that the particle size increases when copper sulphate is used as raw material. Also, the smallest particle size was obtained when copper acetate was used as copper source. So, the particle sizes are about 22-37, 28-44, and 38-50 nm, for S_1, S_2, and S_3, respectively.

3.3. Photodegradation of MG over CuO nanoparticles

The photocatalytic performance of CuO nanoparticle was explored for the degradation of MG at the presence of H_2O_2 (30%, w/w) under blue light illumination. To prepare a 100 ppm MG dye solution, 100 mg of MG powder was poured into 1000 mL of deionized water. The pH amount of the obtained solution was 4. In an ordinary photocatalytic test, certain amount (g) of the as-synthesized CuO photocatalyt (0.02 g, for example) was added into 80 mL of the prepared MG watery solution at the room temperature and sonicated for 10 min in a dark room to set up an adsorption/desorption balance between MG molecules and the surface of the photocatalyst. A short time later, certain volume (mL) of H_2O_2 (0.05 mL, for example) were included into the mixture, while stirring under blue light illumination. The mixture was kept at a constant stirring of 300 rpm at the temperature of the test. The photodegradation yield (%) of MG was calculated by the below equation:

$$\left(\frac{A_0-A_t}{A_0}\right) \times 100 \quad (1)$$

3.4. Photocatalytic process designed by design expert software

Analysts utilize two diverse approaches to get the ideal conditions in chemical responses, to be specific one-at-a-time and experimental design strategies. Up to now, the experimental design method is getting more consideration. Full factorial design is one of the fundamental plans. For a plan, there is k exploring factors and each variable may be set to m particular levels. The number of conceivable combinations of the variables and their settings will at that point be mk. In full factorial strategy, the relation among the variables and reaction is hypothetically modeled. So, it is conceivable for tests to illustrate the yield. Response surface methodology (RSM) may be a numerical and measurable strategy analyzing experimental data by applying an experimental design. RSM utilizing input data, offers the graphical relationship between reaction and

factors, and performs different types of examination [45, 46].

The desirability of the data is checked utilizing ANOVA which needs a few replicate tests. In the present MG degradation process, the goal is to decide how much nanocatalyst should be utilized, and at which time and H_2O_2 volume the degradation should be checked. The reaction was the surrender of degradation (Y%). Distinctive combinations of these components were designed which are detailed in Table 1. A three-level CCD with three components (H_2O_2 (A), catalyst (B) and time (C)) was utilized to examine the impacts of components. The condition of 20 tests designed by CCD associated with to dye degradation yield (reaction (R%)) are also given in Table 1. The actual and coded factors are appeared in Table 2. The ANOVA analyzes the changes and analyzes the centrality of the variables and their intelligent on themselves and other variables. With the assistance of RSM, the goodness of fitting is mentioned in three amounts and interpreted to discover the finest conditions for the method. ANOVA of regression parameters for the quadratic model was computed in Table 3. In the Fisher's F test by the ANOVA investigation, the bigger F-values and the samller P-values show the more critical terms of the model [45, 46].

This proportion is called an F-distribution (F-value), changing from 1 to bigger values. Values far from 1, surpassing from the arranged F-value, give prove against the invalid theory, showing the importance of the relapse parts of the fitted models. In arrange to get the noteworthy and solid show at 95% certainty level, the p-values for the fitted demonstrate and its comparing terms should be less than 0.05. The p-value of the model was samller than 0.05, appearing that the model was desirable at a high certainty level (95%). Another evaluation factor of the fitted model can be carried out utilizing the lack-of-fit test. The assurance coefficients were utilized to specific the quality of fit of quadratic model condition. In this case, R_2 of variety fitting for Y%=78 showed a high degree of relationship between the reaction and the autonomous variables (R^2=0.989). Moreover, the value of (R^2-adj=0.979) coefficient demonstrated high desirability of the proposed model. Moreover, the anticipated R-squared (0.925) was good. It shows the high quality of the created model.

Equation 1 showsthe connection between the components and the yield, Y%, based on the quadratic model:

$$Yield=+63.67+10.34A+15.42B+12.39C+1.62AB+0.8750AC+3.63BC-5.67A^2-9.08B^2-4.22C^2$$

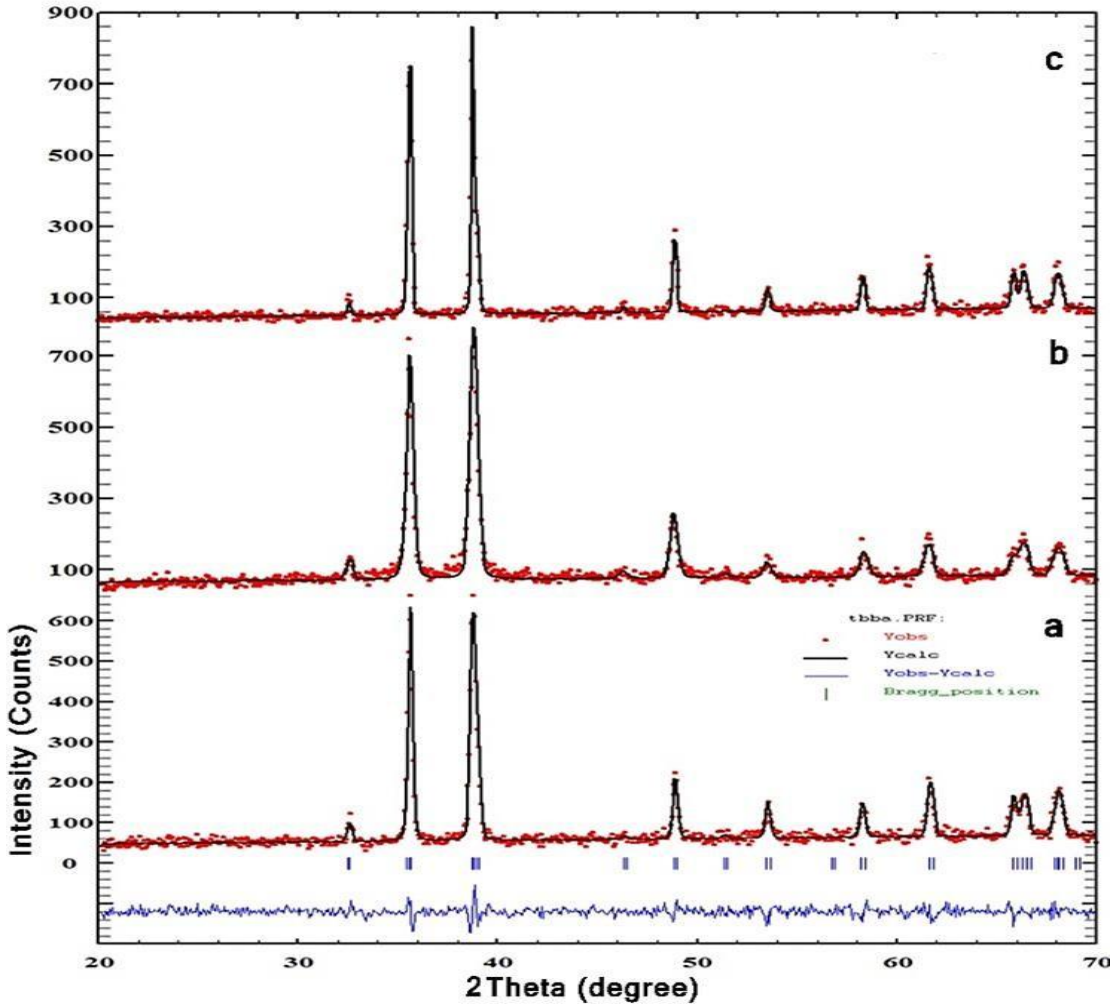

Fig. 1. XRPD patterns of CuO nanomaterials associated with Rietveld analysis data for a) S_1, b) S_2, and c) S_3.

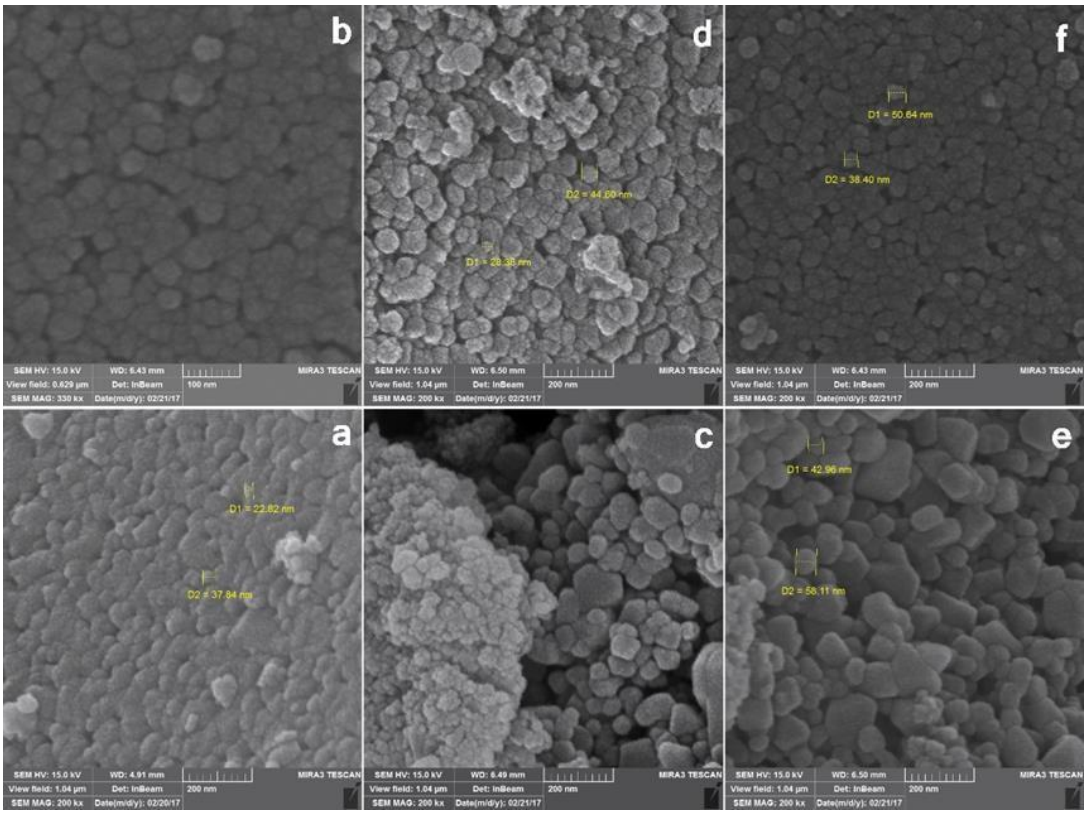

Fig. 2. FESEM images of CuO nanomaterials where a,b) S_1, c,d) S_2, and e,f) S_3.

Table 1. 20 experiments designed by design expert software associated with the obtained degradation yield values.

H_2O_2	Catalyst	Time	Yield
0.06	0.04	20	60
0.03	0.02	20	6
0.045	0.03	40	36
0.03	0.04	60	82
0.045	0.03	40	70
0.06	0.02	60	62
0.045	0.03	40	64
0.06	0.02	20	40
0.03	0.04	20	25
0.045	0.03	40	65
0.06	0.04	60	65
0.03	0.02	60	56
0.045	0.03	0	20
0.045	0.03	40	67
0.075	0.03	40	12
0.045	0.03	40	72
0.045	0.01	40	63
0.045	0.03	80	60
0.015	0.03	40	27
0.045	0.05	40	60

Fig. 3a, shows the plot of the theory versus the experimental degradation yield. This figure demonstrates a great agreement between the theory versus the experimental degradation yield (R^2=0.992) and speaks to the ampleness and desirability of the model. As it is obvious in this figure, the data appear on a straight slant line, illustrating that there's no dispersal. The mandate for selecting the proper control law change based on the leading lambda is given by developing a Box-Cox plot, appeared in Figure 3 b. The least and most extreme values of certainty interim are 0.4 and 1.3, respectively. The certainty amount around this lambda incorporates current point amount of 1, which shows the goodness of the designed model. Normal plot versus studentized residuals calculate plot appeared in Figure 3c confirms the consistency of the model with the test data. Dispersal of residuals is additionally appeared in Figure 3(d-f).

Fig. 4 (a-c) and (d-f) shows the 3D and 2D plots at the optimum conditions obtained by design expert software. The data show that the degradation yield is high when the catalyst amount and H_2O_2 volume are 20 mg and 0.05 mL, respectively. In this case, the degradation yield is 78 %. To show the impacts of the three factors on the photodegradation yield, the response surface methodology (RSM) was utilized. As could be found from Figure 4 c, at a certain response time (C), when H_2O_2 (A) and catalyst (B) amounts increase, dye degradation increases. This shows that, the mass exchange of dye molecule improves the catalytic performance. Besides, increasing the catalyst amount increases the surface area of catalyst for dye molecules and so leads to increase the dye degradation yield. At a certain H_2O_2 volume, increasing the reaction time and catalyst amount increased the reaction yield. Also, the trend is followed by Figure 4 b. But, it is clear that the impacts of the parameters are not equal that can be observed from Figure 4 d-f. The impact of time and catalyst is more than H_2O_2. This is confirmed by the modeled equation.

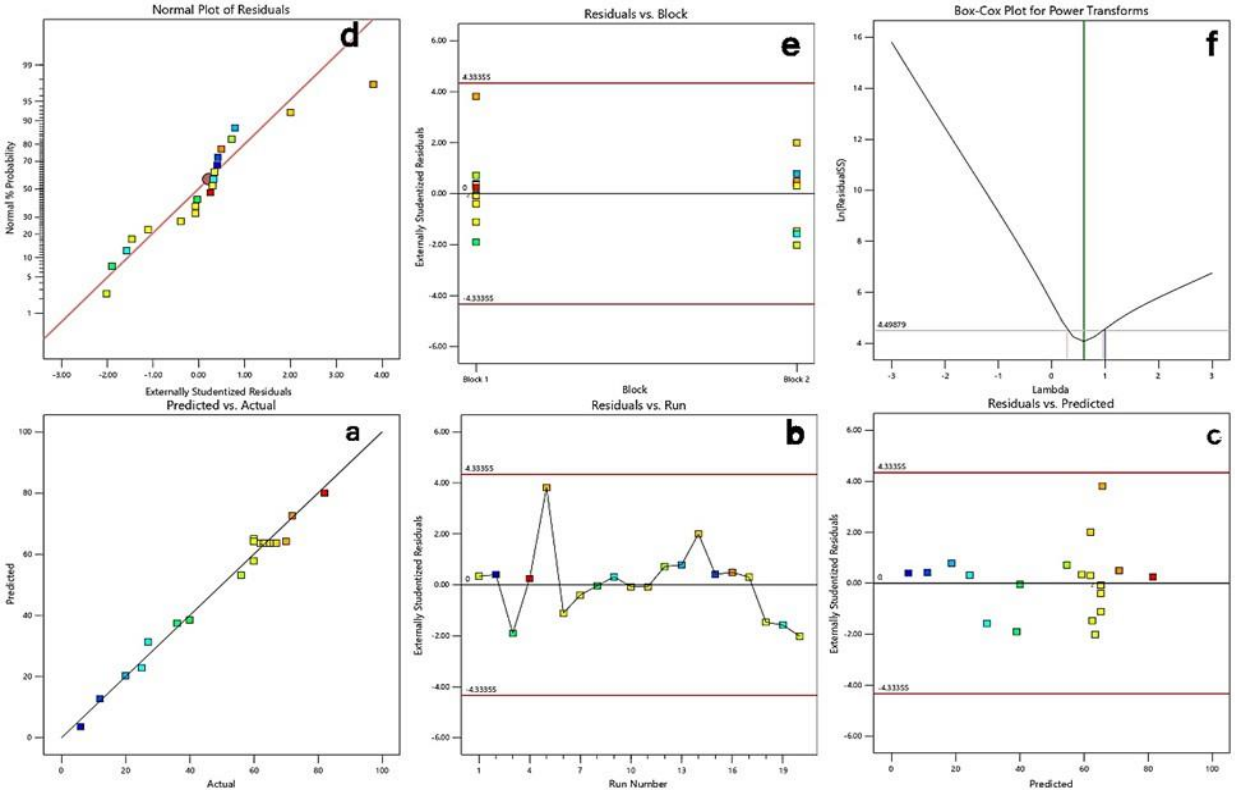

Fig. 3. Output plotted data (a-f) from design expert software using RSM analysis to find the appropriate and sufficient model and confirm the desirability of the proposed final model.

Table 2. Coded and actual parameters for the present photocatalytic process obtained by CCD.

Factor Name	Units	Low Actual	High Actual	Low Coded	High Coded
A	H_2O_2	0.03	0.06	-1	1
B	Catalyst	0.02	0.04	-1	1
C	Time	20	60	-1	1

Fig. 5 outlines the photocatalytic degradation process. Figure 5a presents MG degradation spectra by CuO. The information confirms the high performance of the sample to degrade MG by the mentioned photocatalytic conditions. Figure 5b presents a schematic picture for the degradation of MG at the optimized conditions.

Table 3. Data obtained by ANOVA results for the present photocatalytic reaction.

Source	Sum of Squares	df	Mean Square	F-value	p-value	
Block	118.01	1	118.01			
Model	9000.33	9	1000.04	93.30	< 0.0001	significant
A-H_2O_2	1538.08	1	1538.08	143.50	< 0.0001	
B-Catalyst	3222.37	1	3222.37	300.65	< 0.0001	
C-Time	2082.10	1	2082.10	194.26	< 0.0001	
AB	21.13	1	21.13	1.97	0.1939	
AC	6.13	1	6.13	0.5715	0.4690	
BC	105.13	1	105.13	9.81	0.0121	
A^2	629.33	1	629.33	58.72	< 0.0001	
B^2	1145.78	1	1145.78	106.90	< 0.0001	
C^2	247.55	1	247.55	23.10	0.0010	
Residual	96.46	9	10.72			
Lack of Fit	82.46	5	16.49	4.71	0.0792	not significant
Pure Error	14.00	4	3.50			
Cor Total	9214.80	19				

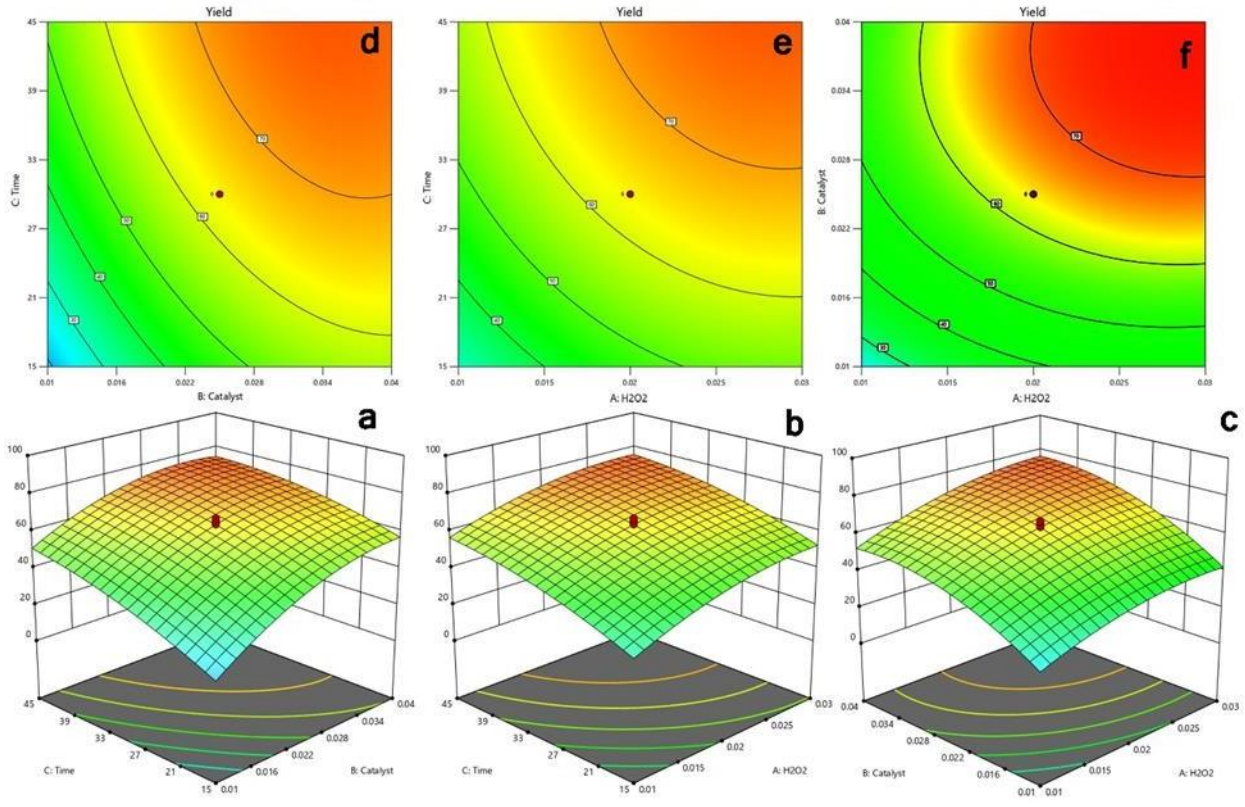

Fig. 4. a-c) 2D and d-f) 3D plots of the obtained data by design expert software.

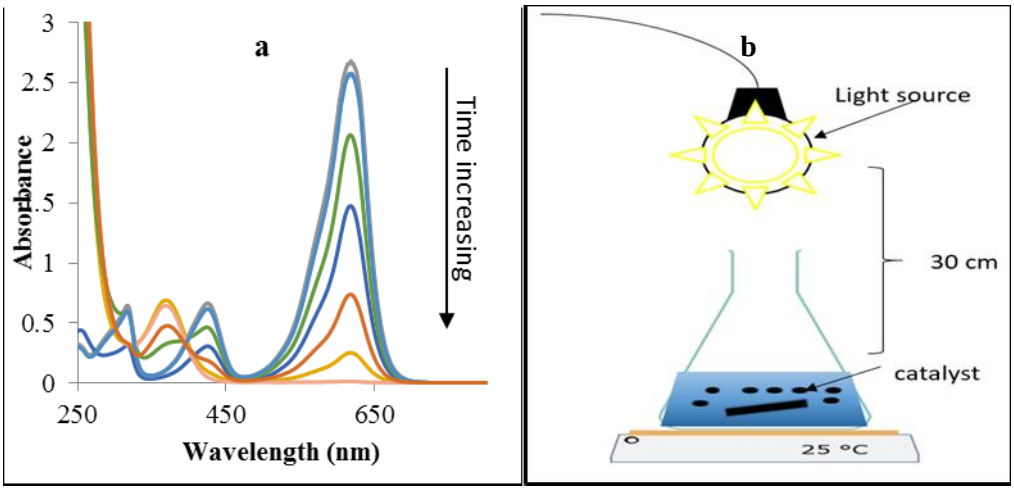

Fig. 5. a) Photodegradation spectra and b) photodegradation process scheme.

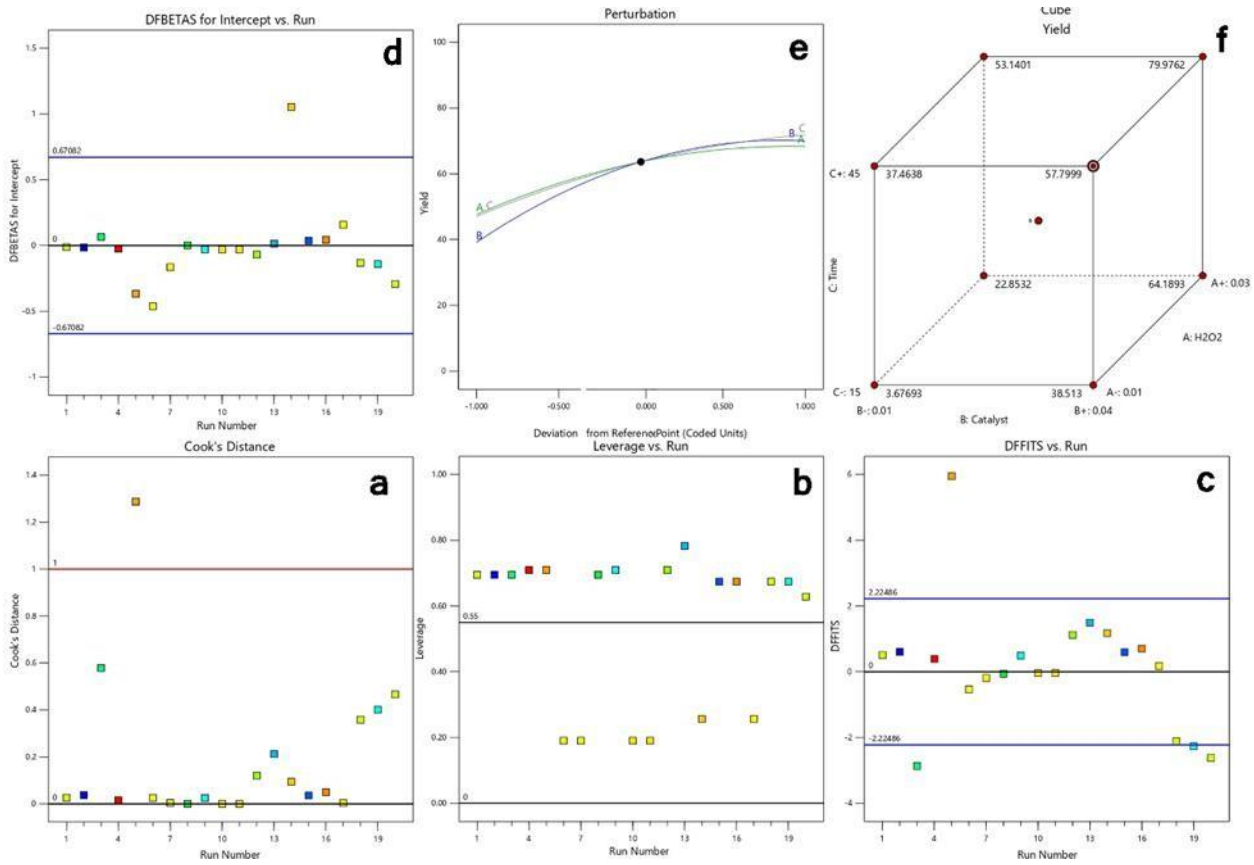

Fig. 6. a) Diagnostic, b) leverage, c) DFFITS, d) DFBETAS versus Run number, e) Perturbation, and f) Cube plots.

Fig. 6a presents Box-Cox plot for control changes remove plot obtained by the Box-Behnken Plan utilizing Cook's separate versus run number, where Cook's remove and studentized residuals outline the ordinary dissemination and the residuals. Box-Cox plot guides us around the choice of the fitting control change of yield factors in required case. The use of a point identical to one indicates that point fits to the recorded data (Figure 6b) and controls the chosen model. All the use values were found in the limits. DFFITS vs Run charts (Figure 6c) clarify the impacts of each designed point on the expected model. DFBETAS vs Run chart decides the effect of each designed point on the coefficients (Figure 6d). The plots displayed in Figure 5e illustrate the comparative impact of all the components at a specific point in the range. This plot makes a difference to recognize the influence of the most important factor on the reaction yield. To show the merit of the present work with the other reported photocatalytic degradation researches, we

present a comparison study among the yield in the present work with the other catalysts (table 4).

Table 4. Comparison study for the degradation efficiency [26].

Catalyst	Condition	Yield (%)
CuO(Present work)	H_2O_2, 20 mg catalyst, 35 min, Blue ligth, 80 mL and 100 ppm MG	78
Carbon/TiO_2	25 ppm MG, 30 min, pH=8	82-100
MoS_2/TiO_2	40 min, sunlight irradiation, 0.1 g catalyst, 10 ppm MG	97
$PbCrO_4$	365 ppm MG, 0.1 g catalyst, 4 h, pH=7.5, visible light, 60 min	90
$Ni_{1-x}Co_xFe_2O_4$	Sunlight, 50 mL solution, 25 ppm catalyst, 1 μM MG, H_2O_2, 15 h	100
Mg-doped TiO_2	Visible light, pH=9, 100 ppm MG	89
ZnO	4h time, 60 ppm MG, pH=7.5, solar radiation	98
$FeSO_4$ -$7H_2O$	10 mM Fe2+, 40 °C, 25.5mM H_2O_2, 10 ppm MG	94
$Sr_2As_2O_7$	H_2O_2, 20 mg catalyst, 33 min, 70 mL of 100 ppm MG, solar light	97

4. Conclusion

In the present study, The Rietveld data obtained from XRD analysis indicated that the cell parameters are a= 4.68244, b=3.42366, c=5.12641 Å and β=99.46° for S_1, a= 4.68073, b=3.42521, c=5.13221 Å and β=99.36° for S_2 and a=4.68233, b=3.42396, c=5.12941 Å and β=99.30º for S_3. FESEM images showed that the synthesized samples had particle morphology with the size range of 20-50 nm. No considerable morphology changes due to changing the raw material type was observed. Design expert software data revealed that the optimum conditions for the corruption of MG were 0.02 g catalyst, 0.05 mL H_2O_2 and 35 min reaction time. The degradation efficiency was 78 %. The concentration and volume of MG solution were 100 ppm and 80 mL, respectively.

References

[1] J. Cao, Y. Wang, T. Ma, Y. Liu, Z. Yuan. "Synthesis of porous hematite nanorods loaded with CuO nanocrystals as catalysts for CO oxidation." Journal of natural gas chemistry 20 (2011) 669-676.

[2] J. Kaneshiro, N. Gaillard, R. Rocheleau, E. Miller. "Advances in copper-chalcopyrite thin films for solar energy conversion." Solar Energy Materials and Solar Cells 94 (2010) 12-16.

[3] Y. Zhang, X. He, J. Li, H. Zhang X. Gao. "Gas-sensing properties of hollow and hierarchical copper oxide microspheres." Sensors and Actuators B: Chemical 128 (2007) 293-298.

[4] B. R. Huang, C. S. Yeh, D. C. Wang, J. T. Tan, J. Sung. "Field emission studies of amorphous carbon deposited on copper nanowires grown by cathodic arc plasma deposition." New Carbon Mater 24 (2009) 97-101.

[5] D. Gupta, S.R. Meher, N. Illyaskutty, Z. C. Alex. "Facile synthesis of Cu2O and CuO nanoparticles and study of their structural, optical and electronic properties." Journal of Alloys and Compounds 743 (2018) 737–745.

[6] M. Kaur, K.P. Muthe, S.K. Despande, S. Choudhury, J.B. Singh, N. Verma, S.K. Gupta, J.V. Yakhmi. "Growth and branching of CuO nanowires by thermal oxidation of copper." Journal of Crystal Growth 289 (2011) 670-675.

[7] W.Narongdet,C.Piyanut, V. Naratip, P. Wisanu. "Sonochemical Synthesis and Characterization of Copper Oxide Nanoparticles." Energy Procedia 29 (2011) 404-409.

[8] M. H. Yamukyan, K. V. Manukyan, S. L. Kharatyan. "Copper oxide reduction by combined reducers under the combustion mode." Chemical Engineering Journal 137 (2008) 636 642.

[9] J. Zhu, D. Li, H. Chen, X. Yang, L. Lu, X. Wang. "Highly dispersed CuO nanoparticles prepared by a novel quick-precipitation method." Materials Letters 58 (2004) 3324-3327.

[10] R. Wu, Z. Ma, Z. Gu, Y. Yan. "Preparationand characterization of CuO nanoparticles with different morphology through a simple quick-precipitation method in DMAC water mixed solvent." Journal of Alloys and Compounds 504 (2010) 45-49.

[11] X.G. Zheng, C.N. Xu, K. Nishikubo, K. Nishiyama, W. Higemoto, W.J. Moon, ... E.S. Otabe. "Finite-size effect on Néel temperature in antiferromagnetic nanoparticles." Physical Review B 72 (2005) 014464.

[12] C.T. Hsieh, J.M. Chen, H.H. Lin, H.C. Shih. "Synthesis of well-ordered CuO nanofibers by a self-catalytic growth mechanism." Applied Physics Letters 82 (2003) 3316–3318.

[13] A. Shui, W. Zhu, L. Xu, D. Qin, Y. Wang. "Green sonochemical synthesis of cupric and cuprous oxides nanoparticles and their optical properties." Ceramics International 39 (2013) 8715–8722.

[14] B. Ebin, Ö. Gençer, S. Gürmen. "Simple preperation of CuO nanoparticles and submicron spheres via ultrasonic spray pyrolysis (USP)." International journal of materials research 104 (2013) 199–206.
[15] X. Gou, G. Wang, J. Yang, J. Park, D. Wexler. "Chemical synthesis, characterisation and gas sensing performance of copper oxide nanoribbons." Journal of Materials Chemistry 18 (2008) 965–969.
[16] J.Y. Li, S. Xiong, J. Pan, Y. Qian. "Hydrothermal synthesis and electrochemical properties of urchin-like core-shell copper oxide nanostructures." The Journal of Physical Chemistry C 114 (2010) 9645–9650.
[17] L. Li, X. Guo, F. Hao, X. Zhang, J.Chen. "Solid-state grinding/low-temperature calcining synthesis of carbon coated MnO_2 nanorods and their electrochemical capacitive property." New Journal of Chemistry 39 (2015) 4731-4736.
[18] S.A. Patil, D.V. Shinde, D.Y. Ahn, D.V. Patil, K.K. Tehare, V.V. Jadhav, J.K. Lee, R.S. Mane, N.K. Shrestha, S.H. Han. "A simple, room temperature, solid-state synthesis route for metal oxide nanostructures." Journal of Materials Chemistry A 2(2014) 13519-13526.
[19] P. Bansal, N. Bhullar, D. Sud. "Studies on photodegradation of malachite green using TiO_2/ZnO photocatalyst." *Desalination and Water Treatment* 12 (2009)108-113.
[20] H. Soni, N.K. JI. "UV light induced photocatalytic degradation of malachite GREEN on TiO_2 nanoparticles." Int. J. Recent Res. Rev. 7(2014) 10-15.
[21] D. Sols-Casados, L. Escobar-Alarcn, M. Fernndez, F. Valencia. "Malachite green degradation in simulated wastewater using Ni_x: TiO_2 thin films." Fuel. 110 (2013) 17-22.
[22] L. Khezami, K.K. Taha, I. Ghiloufi, L. El Mir. "Adsorption and photocatalytic degradation of malachite green by vanadium doped zinc oxide nanoparticles." Water Science and Technology 73 (2016) 881-889.
[23] W.K. Jo, G. T. Parka, R.J. Tayade. "Synergetic effect of adsorption on degradation of malachite green dye under blue LED irradiation using spiral-shaped photocatalytic reactor." Journal of Chemical Technology & Biotechnology 90 (2014) 2280-2289.
[24] H.Y. He. "Photocatalytic degradations of malachite green on magnetically separable $Ni_{1-x}Co_xFe_2O_4$ nanoparticles synthesized by using a hydrothermal process." Amer. Chem. Sci. J. 6 (2015) 58-68.
[25] S. Afshar, H. Samari Jahromi, N. Jafari, Z. Ahmadi M. Hakamizadeh. "Degradation of malachite green oxalate by UV and visible lights irradiation using $Pt/TiO_2/SiO_2$ nanophotocatalyst." Scientia Iranica 18 (2011) 772-779.
[26] S. Khademinia, M. Behzad, L.Kafi-Ahmadi, S. Hadilou. "Solar Light Photocatalytic Degradation of Malachite Green by Hydrothermally synthesized strontium arsenate nanomaterial through response surface methodology." Zeitschrift für anorganische und allgemeine Chemie 644 (2018) 221-227.
[27] B. Azari, A. Pourahmad, B. Sadeghi, M. Mokhtary. "Preparation and photocatalytic study of SiO_2/CuS core-shell nanomaterial for degradation of methylene blue dye." Nanoscale 3(2019) 103-114.
[28] R. Hajavazzade, M. Kargar Razi, A.R. Mahjoub. "Synthesis and characterization of $Mg_{1-x}Ni_xAl_2O_4$ and their photocatalytic behaviors towards Congo red under UV light irradiation." International Journal of Nano Dimension. 12 (2021) 67-75.
[29] S.K. Blourfrosh, K. Mahanpoor. "Preparation, characterization and photocatalytic performance of nano α-Fe_2O_3 supported on metal organic framework of Cd(II) for decomposition of Cefalexin aqueous solutions." International Journal of Nano Dimension 12 (2021) 113-127.
[30] V.G. Shtamburg, V.V. Shtamburg, E.A. Klots, A.A. Anishchenko, A.V. Mazepa, S.V. Kravchenko. "Nucleophilic Substitution In N-Alkoxy-N-Chlorocarbamates As A Way To N-Alkoxy-N', N', N'-Trimethylhydrazinium Chlorides." European Chemical Bulletin, 9 (2020) 28-32.
[31] O.V. Mikhailov, D.V. Chachkov. "Molecular Structure Models Of Al2ti3 And Al2v3 Clusters According To Dft Quantum-Chemical Calculations." European Chemical Bulletin 9 (2020) 62-68.
[32] V. Bakhtadze, V. Mosidze, T. Machaladze, N. Kharabadze, D. Lochoshvili, M. Pajishvili, … , N. Mdivani. "Activity Of Pd-Mnox/Cordierite (Mg, Fe) 2al4si5o18) Catalyst For Carbon Monoxide Oxidation." European Chemical Bulletin 9 (2020) 75-77.
[33] J.P. Sonar, S.D. Pardeshi, S.A. Dokhe, K.R. Kharat, , A.M. Zine, , L. Kótai, ... , S.N. Thore. "Synthesis And Anti-Proliferative Screening Of Newthiazole Compounds." European Chemical Bulletin 9 (2020) 132-137.
[34] P.G. Pathare, S.U. Tekale, M.G. Damale, J.N. Sangshetti, R.U. Shaikh, L. Kótai, R.P.P. Silaev. "Pyridine And Benzoisothiazole Based Pyrazolines: Synthesis, Characterization, Biological Activity, Molecular Docking And Admet Study." European Chemical Bulletin 9 (2020) 10-21.
[35] H. Watandost, J. Achak, A. Haqmal. "Oxidation Of Hydrogels Based Of Sodium Alginate And Mno2 As Catalyst." International Journal Of Innovative Research And Scientific Studies 4 (2021) 191–199.
[36] M. Bashirzadeh, "Green Synthesis Of Quinoxaline Derivatives At Room Temperature In Ethylene Glycol With H2so4/Sio2 Catalyst." European Chemical Bulletin 9 (2020) 33-37.
[37] D.V. Chachkov, V.M. Oleg "Novel Modifications Of Elemental Nitrogen And Their Molecular Structures–A Quantum-Chemical Calculation." European Chemical Bulletin 9 (2020) 78-81.
[38] O.H. Oladimeji, M.A. Anwana, E.E. Attih, D.E. Effiong. "3, 4, 5-Trihydroxycyclohexyl Methanol-A New Reduced Derivative From Structural Activity Relationship Studies (Sars) On Gallic Acid." European Chemical Bulletin 9 (2020) 103-106.
[39] S.B. Landge, S.B. Dahale, S.J. Devadhe, D.G. Deshmukh, P.V. Solanki, S.A. Jadhav, ... R.P. Pawar. "Separation And Quantification Of Structurally Similar Impurities By Hplc Method Of Vortioxetine Hydrobromide-An Antidepressant Drug." European Chemical Bulletin 9 (2020)114-118.
[40] Z. Shehu, W.L. Danbature, B. Magaji, M.M. Adam, M.A. Bunu, A.J. Mai, Y. Mela. "Green Synthesis And Nanotoxicity Assay Of Copper-Cobalt Bimetallic

Nanoparticles As A Novel Nanolarvicide For Mosquito Larvae Management." The International Journal Of Biotechnology 9 (2020) 99-104.

[41] I. Choudhuri, S. Panja, K. Khanra, N. Bhattacharyya. "Identification And Characterization Of A Pb, Cu And Antibiotic Resistant Bacteria From Soil Of Industrial Wastewater Ground." International journal of Advanced Biological and Biomedical Research 4 (2016) 194-201.

[42] H. Esmaeilzadeh, E. Fataei, H. Saadati. "Nh3 Removal From Sour Water By Clinoptilolite Zeolite: A Case Study Of Tabriz Refinery." Chemical Methodologies 4 (2020) 754-773.

[43] A. El-Khateeb, M.H. Mahmoud, M. Fakih. "Comparative Study On Different Horizontal Subsurface Substrates In Flow Wetlands." Progress In Chemical And Biochemical Research 2 (2019) 20-23.

[44] A. Gorgizade, M.B. Marzouni, N.J. Haghighifard, M. Rafiei, M. Esmaeili. "Water Quality Evaluation Of Bamdezh Wetland Using Combination Of Nsfwqi And Geographic Information System." International Journal of Advanced Biological and Biomedical Research 2 (2014) 1454-1467.

[45] S.S. Hosseiny Davarani, Z. Rezayati Zad, A.R. Taheri, N. Rahmatian. "Highly selective solid phase extraction and preconcentration of Azathioprine with nano-sized imprinted polymer based on multivariate optimization and its trace determination in biological and pharmaceutical samples." Materials Science and Engineering: C 71 (2017) 572–583.

[46] F. Abdollahi, A. Taheri, M. Shahmari, "Application of selective solid-phase extraction using a new core-shell-shell magnetic ionimprinted polymer for the analysis of ultra-trace mercury in serum of gallstone patients." Separation Science and Technology 55 (2020) 2758-2771.